Alzheimer's & Dementia®
THE JOURNAL OF THE ALZHEIMER'S ASSOCIATION

RESEARCH ARTICLE

Synaptic resilience is associated with maintained cognition during ageing

Declan King[1] | **Kris Holt**[1] | **Jamie Toombs**[1] | **Xin HE**[1] | **Owen Dando**[1] | **Judith A Okely**[2] | **Makis Tzioras**[1] | **Jamie Rose**[1] | **Ciaran Gunn**[1] | **Adele Correia**[1] | **Carmen Montero**[1] | **Hannah McAlister**[1] | **Jane Tulloch**[1] | **Douglas Lamont**[3] | **Adele M Taylor**[2] | **Sarah E Harris**[2] | **Paul Redmond**[2] | **Simon R Cox**[2] | **Christopher M Henstridge**[4] | **Ian J Deary**[2] | **Colin Smith**[5] | **Tara L Spires-Jones**[1]

[1]UK Dementia Research Institute and Centre for Discovery Brain Sciences at the University of Edinburgh, Edinburgh, UK

[2]Lothian Birth Cohorts, Department of Psychology, University of Edinburgh, Edinburgh, UK

[3]FingerPrints Proteomics Facility, School of Life Sciences, University of Dundee, Dundee, UK

[4]Systems Medicine, School of Medicine, University of Dundee, Dundee, UK

[5]Neuropathology, Centre for Clinical Brain Sciences, University of Edinburgh, Edinburgh, UK

Correspondence
Tara L Spires-Jones, UK Dementia Research Institute and Centre for Discovery Brain Sciences at the University of Edinburgh, 1 Goerge Square, Edinburgh, EH8 9JZ, UK.
Email: Tara.spires-jones@ed.ac.uk

Abstract

Introduction: It remains unclear why age increases risk of Alzheimer's disease and why some people experience age-related cognitive decline in the absence of dementia. Here we test the hypothesis that resilience to molecular changes in synapses contribute to healthy cognitive ageing.

Methods: We examined post-mortem brain tissue from people in mid-life ($n = 15$), healthy ageing with either maintained cognition ($n = 9$) or lifetime cognitive decline ($n = 8$), and Alzheimer's disease ($n = 13$). Synapses were examined with high resolution imaging, proteomics, and RNA sequencing. Stem cell-derived neurons were challenged with Alzheimer's brain homogenate.

Results: Synaptic pathology increased, and expression of genes involved in synaptic signaling decreased between mid-life, healthy ageing and Alzheimer's. In contrast, brain tissue and neurons from people with maintained cognition during ageing exhibited decreases in synaptic signaling genes compared to people with cognitive decline.

Discussion: Efficient synaptic networks without pathological protein accumulation may contribute to maintained cognition during ageing.

KEYWORDS
ageing, Alzheimer's, cognition, synapse

1 | BACKGROUND

Cognitive decline is described as one of the most feared aspects of the ageing process.[1-4] As well as cognitive decline being common during ageing, age is the most important risk factor for Alzheimer's disease (AD). Region-specific synapse loss has been observed in post-mortem studies of aged human brain and in animals similar changes are associated with cognitive decline.[5] In AD, synapse loss also correlates strongly with cognitive decline[6-8] and we have observed that synaptic accumulation of pathological forms of amyloid beta (Aβ) and tau are associated with synapse loss in AD brain.[9-11] In model systems, we and others have observed that altered synaptic signaling downstream of Aβ and tau cause cognitive decline in ageing animals.[12] Several well-characterized cohorts have been used to study brain changes associated with cognitive ageing including the Religious Orders Study, Rush Memory and Ageing Project and the Cognitive Function and Ageing Studies.[13-16] These and other studies highlight the importance of different responses to pathological protein accumulation and both the genetic and environmental risk factors associated with age-related cognitive decline. However, significant gaps in knowledge remain including understanding brain changes associated with cognitive change over a large portion of the lifetime (starting in childhood) and detailed analysis of synapse density and protein composition at high resolution previously prevented by technical limitations. Here we address some of these knowledge gaps using a combination of advanced techniques and brain donations from the participants in the Lothian Birth Cohort 1936 (LBC1936), a well-characterized cohort studying cognitive ageing.[17-21] LBC1936 participants took a version of the Moray House Test No. 12 (MHT) of general intelligence at age 11 and have participated since the age of 70 in a longitudinal study of cognitive ageing. Using brain samples and induced pluripotent stem cell (iPSC) derived neurons derived from this unique cohort alongside brain tissue donated from middle-aged people who died from non-neurological conditions, and people who died with AD,[22,23] we have conducted an in-depth study of synaptic pathology and molecular composition to study synaptic changes associated with resilience to cognitive decline in ageing.

2 | METHODS

Full methods details can be found in the Supplementary Methods File. Abbreviated methods follow.

2.1 | Subjects

Brain tissue and blood donations have been reviewed and approved for use by the Edinburgh Brain Bank ethics committee and the Academic and Clinical Central Office for Research and Development, a joint office of the University of Edinburgh and NHS Lothian (approval 15-HV-016). Three groups of participants were included: (1) mid-life controls (age range 19 to 58, $n = 15$); (2) healthy agers from LBC1936 (age range 77 to 84, $n = 18$) and (3) Alzheimer's disease (age range

RESEARCH IN CONTEXT

- **Systematic Review**: Authors reviewed relevant literature using PubMed searches. There is a wide literature supporting synapse loss as an important mediator of cognitive decline in Alzheimer's disease and some region-specific synaptic changes occur during ageing. Less is known about how synaptic resilience may protect against cognitive decline. References are cited in the introduction and discussion.
- **Interpretation**: Our findings support the idea that accumulation of pathology in synapses and decreased expression of genes involved in synaptic function are associated with Alzheimer's disease, however in healthy ageing without dementia, a paradoxical dampening of genes involved in synaptic signalling is associated with protection from cognitive decline.
- **Future Directions**: Using the stem cell-derived neuronal models presented in this paper and other model systems, future work will be able to search for interventions to reverse molecular changes discovered here that are associated with cognitive decline in ageing and Alzheimer's disease.

61 to 95, $n = 13$). Table 1 shows summary demographics. Inclusion and exclusion criteria for each group is as follows: mid-life controls – within age range specified with no neurological or psychiatric diagnoses and no neuropathological diagnoses at autopsy; healthy agers – participation in the Lothian Birth Cohort 1936 with no dementia diagnosis and no severe neurodegeneration-associated pathology (Braak stage < 5); Alzheimer's disease – clinical dementia diagnosis and confirmed neuropathological diagnosis of AD. Detailed information for each participant is included in DOI Methods Table S1.

2.2 | Cognitive testing

The Moray House Test (MHT) of general intelligence was administered to LBC1936 participants at age 11 and at ages 70, 76, and 79. Longitudinal MHT scores were used to sub-categorize donors of the available post-mortem brain tissue samples from our healthy agers (HA) into either Lifetime cognitive resilient (LCR) or Lifetime cognitive decline (LCD) groups (note, cognitive data was missing from one HA participant). This classification was achieved by plotting age-adjusted MHT scores from age 11 against the mean of older-age-adjusted MHT scores from ages 70 and 76 from all healthy agers in the cohort ($n = 641$). Donors of post-mortem samples were then plotted on this lifetime cognitive scale, where samples above the regression line were defined as LCR ($n = 9$) and those below were defined as LCD ($n = 8$). Methods Table S2 shows summary demographics.

TABLE 1 Summary demographic data of human brain tissue donors

Age (Years)	Midlife (ML) (N = 15)	Healthy Agers (HA)* (N = 18)	Alzheimer's Disease (AD) (N = 13)	Overall (N = 46)
Mean (SD)	42.7 (9.41)	80.7 (2.33)	80.8 (11.0)	68.3 (19.6)
Median (Min, Max)	46.0 (19.0, 58.0)	80.0 (77.0, 85.0)	84.0 (61.0, 95.0)	79.0 (19.0, 95.0)
Sex				
M	10 (66.7%)	11 (61.1%)	7 (53.8%)	28 (60.9%)
F	5 (33.3%)	7 (38.9%)	6 (46.2%)	18 (39.1%)
Brain pH				
Mean (SD)	6.26 (0.218)	6.05 (0.177)	6.12 (0.186)	6.14 (0.210)
Median (Min, Max)	6.27 (5.69, 6.73)	6.01 (5.76. 6.50)	6.10 (5.82, 6.55)	6.13 (5.69, 6.73)
PMI (Hours)				
Mean (SD)	86.7 (22.9)	60.1 (23.7)	83.4 (17.8)	75.3 (24.8)
Median (Min, Max)	94.0 (47.0, 126)	64.5 (30.0, 95.0)	80.0 (49.0, 112)	74.5 (30.0, 126)
Brain Weight (g)				
Mean (SD)	1430 (111)	1320 (98.1)	1240 (134)	1330 (134)
Median (Min, Max)	1460 (1200. 1570)	1320 (1160, 1500)	1230 (1030, 1440)	1330 (1030, 1570)
APOE Genotype**				
2/3	0 (0%)	3 (16.7%)	1 (7.7%)	4 (8.7%)
3/3	6 (40.0%)	12 (66.7%)	3 (23.1%)	21 (45.7%)
3/4	9 (60.0%)	3 (16.7%)	9 (69.2%)	21 (45.7%)
Braak Stage				
0	15 (100%)	2 (11.1%)	0 (0%)	2 (4.3%)
1	0 (0%)	6 (33.3%)	0 (0%)	6 (13.0%)
2	0 (0%)	6 (33.3%)	0 (0%)	6 (13.0%)
3	0 (0%)	1 (5.6%)	0 (0%)	1 (2.2%)
4	0 (0%)	2 (11.1%)	0 (0%)	2 (4.3%)
5	0 (0%)	0 (0%)	0 (0%)	0 (0%)
6	0 (0%)	1 (5.6%)	13 (100%)	14 (30.4%)
Thal Stage				
0	13 (86.7%)	3 (16.7%)	0 (0%)	3 (6.5%)
1	2 (13.3%)	8 (44.4%)	0 (0%)	8 (17.4%)
2	0 (0%)	2 (11.1%)	0 (0%)	2 (4.3%)
3	0 (0%)	2 (11.1%)	1 (7.7%)	3 (6.5%)
4	0 (0%)	2 (11.1%)	2 (15.4%)	4 (8.7%)
5	0 (0%)	1 (5.6%)	10 (76.9%)	11 (23.9%)
6	0 (0%)	0 (0%)	0 (0%)	0 (0%)

*HA subset of LBC1936 Cohort.
**No 2/4 or 4/4 APOE genotypes.

2.3 | Tissue preparation

Protocols for post-mortem brain processing were detailed previously.[23] Brain tissues were processed for biochemistry and synaptoneurosome preparation and embedding for histopathology (IHC) and array tomography (AT) (Figure S1). Brain regions studied included: primary visual cortex (BA17); middle temporal gyrus (BA20/21); anterior cingulate cortex (BA24); dorsolateral prefrontal cortex (BA46) and posterior hippocampus. For AT, RNA-seq and proteomics, two of these brain regions BA17 and BA20/21 were investigated.

2.4 | Synaptoneurosome preparation

Total tissue homogenate and synaptoneurosome fractions were prepared using frozen tissue samples with minor adjustments as previously described.[24] Tissue was homogenized and passed through an

80 μm nylon net filter (Millipore) to generate the total homogenate. Half of the total homogenate was passed through a Millex-SV 5 μm membrane filter (Millipore) then centrifuged at 1000 × g for 5 min to generate synaptoneurosome pellets. Pellets were reconstituted and homogenized with 450 μL buffer. Protein quantification was carried out using the micro Bicinchoninic acid assay (Pierce, UK).

2.5 | Label-Free quantitative (LFQ) mass spectrometry (MS)

Sample preparation for LFQ-MS was carried out based on previous proteomic workflows.[25,26] Peptides generated from total homogenate and synaptoneurosome samples were analyzed by MS using a Q-Exactive-HF (Thermo Scientific) mass spectrometer coupled with a dionex Ultimate 3000 RSLCnano (Thermo Scientific). Protein differential expression analysis was performed using DEP (Differential Enrichment analysis of Proteomics data; R package version 1.6.1).

2.6 | SDS-PAGE and immunoblotting

SDS-PAGE and immunoblotting was performed as described previously.[23] Primary antibodies used for immunoblotting are shown in Supplementary methods (Methods Table S3). Proteins were detected on an Odyssey system using 680 and 800 IR dye secondary antibodies. Total protein stains were performed with Ponceau S and/or REVERT total protein stains.

2.7 | RNA extraction and analysis

mRNA was extracted from both total homogenate and synaptoneurosome samples using the RNeasy Plus Micro Kit (Qiagen). Illumina libraries were prepared using TruSeq mRNA Sample Prep Kit. Illumina sequencing was carried out on a NovaSeq platform using 50 base paired-end reads. Differential expression analysis was performed using DESeq2 (R package version 3.6.1)[27] followed by gene set analysis using Camera[28] from the limma R package (version 3.40.6)[29] and Gene Ontology enrichment analysis using topGO (R package version 2.36;[30]. qPCR was performed in an CFX96 Real-time system (Bio-Rad) using BRYT Green Dye (Promega) and the GoTaq 1-Step RT-qPCR kit (Promega).

2.8 | Histopathology

Fresh post-mortem tissue blocks were fixed in 10% formalin, dehydrated and paraffin embedded. Tissue sections were cut on a Leica microtome at 4 μm thickness and processed for immunohistochemistry using the Novolink Polymer Detection Kit (Leica, Figure S1).

All immunolabelled sections were assessed blind to case information and stain burdens were calculated using Stereo Investigator (MBF Bioscience).

2.9 | Array tomography

Fresh brain samples were fixed in 4% paraformaldehyde, dehydrated, and embedded in LR white resin as previously described.[22] Ribbons of 70 nm serial sections were cut on an ultramicrotome (Leica) then stained with immunofluorescence and imaged using an AxioImager Z2 with an 63 × 1.4 NA objective. Array tomography images were processed with an in-house image analysis pipeline (Figure S1).

2.10 | iPSC-neuron culture

We reprogrammed peripheral blood mononuclear cells (PBMCs) from the LBC1936 cohort as detailed in.[31] iPSCs were differentiated to glutamatergic cortical neurons by dual SMAD inhibition, following a protocol adapted from Shi et al.[32] Neurons were cultured to 60 days post final passage in vitro, exposed to Aβ+ or Aβ- homogenate for 48 h, then samples collected for RNA extraction or fixed for imaging. Stained neurons were imaged on a Leica TCS confocal microscope with an oil immersion 63x objective. Generation and immunodepletion of human brain homogenate for treating iPSC derived neurons was conducted following a protocol adapted from Hong et al.[33] Human superior temporal cortex was homogenized, centrifuged, and dialyzed. Homogenates were immunodepleted for Aβ using 4G8 antibody or mock immunodepleted with mouse serum. Concentration of Aβ1-42 in Aβ+ and Aβ- homogenate was quantified by ELISA (WAKO, 296-64401).

2.11 | Statistics and data sharing

Group comparisons including variables Cohort (or cognitive status), Sex, post-mortem interval (PMI), APOE status, Plaque present/absent were analyzed using Linear mixed effects models including case as a random effect to account for multiple measures per case. Specifically for array tomography, tissue sample was nested within case as a random effect and experimenter was included as a random effect as more than one person collected the data. Where data failed to meet model assumptions, data were transformed via Tukey's Ladder of Power. ANOVA with Satterthwaite correction was performed on the linear mixed effects models and post-hoc Tukey-corrected comparisons were made between groups. All analyses were performed using R Studio[34] (R 4.4.1). All software macros used in this paper are available at https://github.com/Spires-Jones-Lab, R scripts, and analyzed data spreadsheets containing anonymized data are freely available on Edinburgh DataShare at https://doi.org/10.7488/ds/3777 and raw images associated with the study can be

3 | RESULTS

3.1 | Synaptic pathology and gliosis increase from mid-life to ageing to Alzheimer's disease

Synapses from two brain regions BA20/21 and BA17 (middle/inferior temporal gyrus and primary visual cortex) were stained for presynapses (synaptophysin), postsynapses (PSD95), tau (total tau), and oligomeric Aβ (OC, Figure 1). A mean of 341 million paired synapses (SD 53.6 million) were analyzed per cohort. There is a decrease in synapse density between mid-life (ML) and AD in both regions and ML and healthy agers (HA) in BA17 (post/pre-synaptic pairs defined as a positive pre and post-synaptic puncta within 0.5 μm distance) (Figure 1B). Three-dimensional reconstructions of array tomography image stacks show accumulation of Aβ (Figure 1C) and total tau (Figure 1D) within synapses. Quantification of co-localization reveals that Aβ accumulates within paired pre-synaptic terminals increasing from mid-life to healthy ageing to AD. Cohort and presence of plaque in the image stack were associated with a significant increase in the proportion of synapses with Aβ (Figure 1E). Similar results are observed when we examine post-synaptic terminals containing Aβ (Figure 1F). We observe total tau accumulating in pre-synaptic terminals (Figure 1G) with more tau in AD pre-synapses than in healthy ageing or mid-life and more in BA20/21 than BA17. Similar effects are observed for total tau accumulation in post-synaptic densities (Figure 1H). Using standard immunohistochemistry on paraffin sections, we measured the accumulation of amyloid plaques, gliosis and P-Tau in five brain regions (BA20/21 - middle/inferior temporal gyrus, BA17 - primary visual cortex, BA24 – cingulate cortex, BA46 – dorsolateral prefrontal cortex, and hippocampus). Aβ accumulation increased between ML, HA and AD post-mortem brains (Figure S2A). Stereological quantification validated a step-wise increase in Aβ between ML, HA, and AD samples (Figure S2B) and both cohort and regional effects were evident and highest in BA24 AD brains. There were also differences in Aβ burdens between males and females, and *APOE4* carriers and non-carriers. Stereological quantification of reactive astrocyte (GFAP) burdens shows an increase between ML, HA, and AD (Figure S2C). There was a main effect of cohort and region and post-hoc comparisons showed a significant increase in GFAP burden in AD in comparison to HA or ML in BA20/21.

Microglial (CD68) burden increased between ML, HA, and AD and varied between brain regions with most significant changes occurring in BA20/21 and BA46 (Figure S2D). P-Tau burdens increased between ML, HA, and AD samples (Figure S2E) where both cohort and regional effects were evident. P-Tau was highest in BA20/21 and hippocampal AD brains. There was also an effect of *APOE* carriers and non-carriers. Together, these data indicate that synapses are lost between midlife, ageing, and AD alongside an increase in gliosis and synaptic accumulation of pathological proteins.

3.2 | Molecular changes in synapses in age and Alzheimer's disease

Using RNA sequencing, we observe thousands of differentially expressed gene transcripts (DEG's) in synapses from BA20/21 temporal cortex samples from people with AD compared to mid-life controls (9671 DEG's) and when comparing healthy ageing people without dementia (HA) to mid-life controls (5801 DEG's, Figure 2A-B). Two hundred and ninety three genes were differentially expressed between HA and AD subjects (Figure 2C). Similarly, numerous transcriptional changes were also observed in BA17 region and in total homogenate preparations between AD/HA and ML, but there were no differences in gene expression in BA17 between healthy ageing and AD (DOI Table S2). Canonical pathways predicted to be inhibited (decreased) in AD or HA in comparison to ML were associated with neurotransmission and memory whilst stress and immune response pathways were predicated to be activated or increased (Figure 2D). In HA versus AD, there were increases in synaptic function pathways and a decrease in one stress response pathway, EIF2 signaling (Figure 2E). These data compliment Gene-set analysis (GSA) datasets (DOI Folder S1-2) generated independently of IPA and based on gene sets with shared biological and functional properties. Using the SynGo curated database[35] (https://www.syngoportal.org/index.html) specifically designed as a resource for synaptic specific associated genes, we observe approximately equal numbers of changes in genes important in pre and post synaptic function (Figure 2F-H). Fewer differentially expressed proteins (DEP's) were identified (DOI Table S2) when comparing the same tissues at the proteomic level (Figure S3A-C). A subset of DEG's identified from RNA-seq datasets were validated by RT-qPCR (Figure S3D-J) namely, Related Ras small GTPase (*RRAS*); Inositol 1,4,5-trisphosphate (*ITPR1*), Glutamate decarboxylase 2 (*GAD2*); Synaptosomal-Associated Protein, 25 kDa (*SNAP-25*), Transmembrane 4 L Six Family Member 1 (*TM4SF1*) and Synatotagamin-1 (*SYT1*). Overall, all RT-qPCR expression profiles matched RNA-seq directional changes (DOI Table S3). A subset of DEP's namely, Clusterin (CLU), Stomatin (STOM) and Vimentin (VIM) identified from proteomics datasets were validated by immunoblotting (Figure S3K-N). Collectively, all immunolabelling blot expression profiles matched proteomic directional changes (Table S3).

3.3 | Cognitive resilience in healthy ageing is associated with lower glial burdens and dampened synaptic activity pathways

In addition to examining differences between healthy ageing, mid-life, and Alzheimer's disease, we stratified healthy ageing participants into categories based on their lifetime cognitive trajectories. To determine cognitive ageing status as either lifetime cognitive resilience (LCR) or lifetime cognitive decline (LCD), we plotted the age adjusted intelligence test scores at age 11 years versus the mean of those taken at age 70 and 76 for all participants in the LBC1936 study with relevant data (Methods Figure S1). Brain donors in this study who fall above the population regression line were considered resilient (*n* = 9)
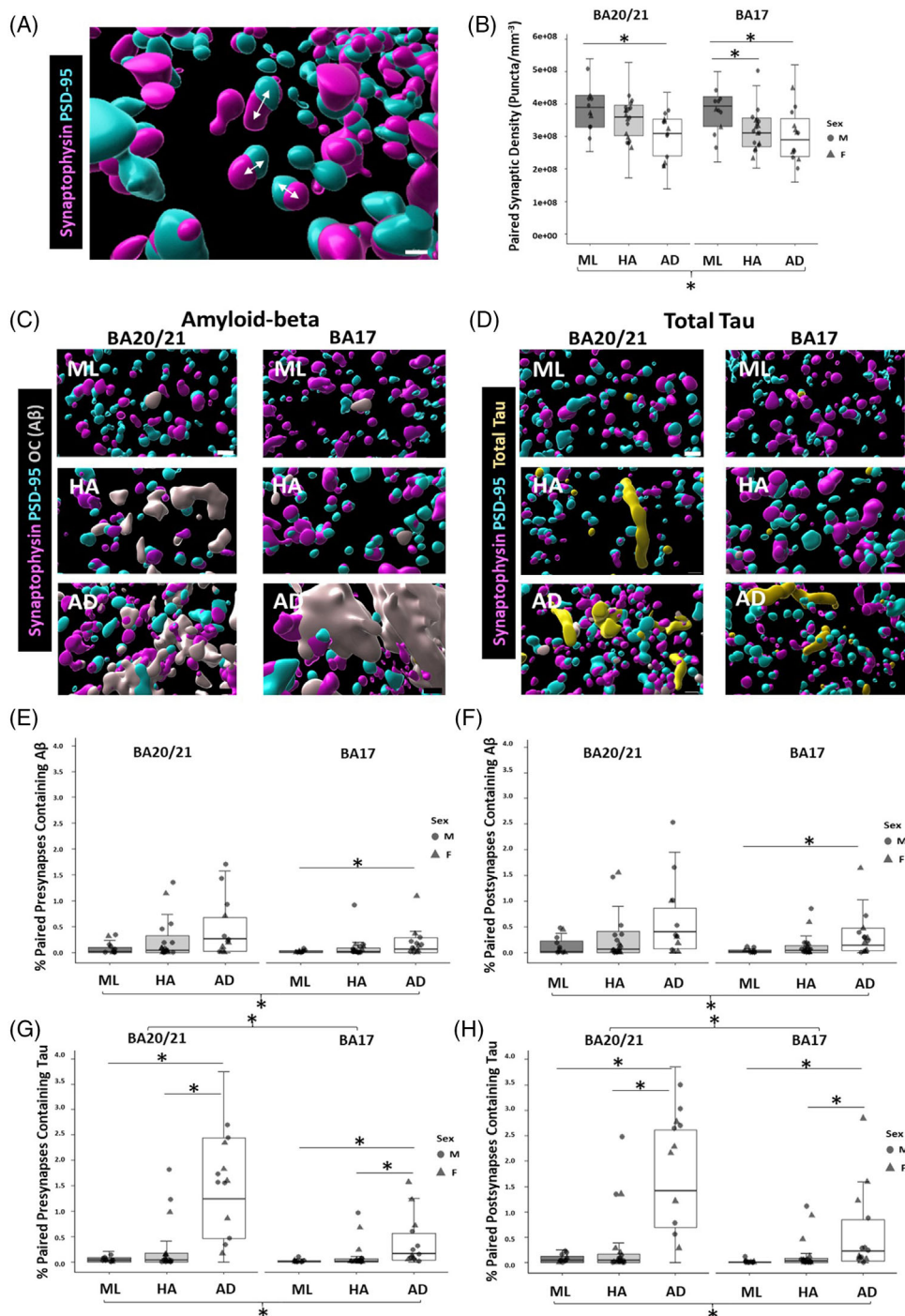
FIGURE 1 High-resolution array tomography (AT) reveals synaptic pathology in ageing and AD. (A) Synapses were quantified from AT image stacks and counted as a synaptic pair if the centroid of the presynaptic object (synaptophysin, magenta) was within 0.5 mm of the nearest postsynaptic object (PSD95, cyan). Arrows show examples of synaptic pairs. (B) The density of paired synapses decreases between mid life (ML), healthy ageing (HA), and Alzheimer's disease (AD) and a linear mixed effects model followed by ANOVA shows there was an effect of cohort F[2,36.79] = 7.02, p = 0.002. There were no differences in synapse density between males and females, or *APOE4* carriers and non-carriers. Pairwise post-hoc comparisons showed synapses were significantly decreased in the AD cohort in comparison to ML and this was evident in both brain regions (BA20/21, t ratio = 3.02; p = 0.005, d = 68; BA17, t ratio = 3.04; p = 0.009, d = 59). Synapses were also decreased in HA in comparison to ML in BA17 (t ratio = 2.76; p = 0.02, d = 57). We examined the synaptic localization of Aβ (grey, C) and tau (yellow, D). In presynaptic terminals, there was a trend towards an increase in Aβ accumulation between midlife, healthy agers, and AD (E, F[2,34.95] = 3.30, p = 0.04) and a significant increase in presynaptic Aβ in regions containing plaques (F[2,164.15] = 15.39, p < 0.0001). Pairwise post-hoc comparisons showed a significant increase in Aβ accumulation in AD BA17 (t ratio = 2.60; p = 0.03, d = 69). In post-synaptic terminals, there was a significant increase in accumulation of Aβ between ML, HA, and AD (F, F[2,37.25] = 4.39, p = 0.01) and a significant increase in postsynaptic Aβ in regions containing plaques (F[2,157.72] = 12.23, p < 0.0001). Pairwise post-hoc comparisons showed a significant increase in Aβ accumulation in AD BA17 (t

and those below were categorized as having lifetime cognitive decline (*n* = 8). Array tomography analysis revealed no differences in synapse densities between cognitive groups however densities were lower in BA17 than in BA20/21 (Figure 3A, B). These data indicate the possibility that other mediators may be affecting cognitive performance in ageing. Next, we investigated whether Aβ and/or tau co-localization differs in those considered cognitively resilient compared to people falling into the lifetime cognitive decline category. Three-dimensional reconstructions of array tomography image stacks shows no difference in synaptic accumulation of Aβ or tau in LCR versus LCD groups with both cognitive groups displaying more synaptic pathology in BA20/21 than BA17 (Figure 3C-F). Stereological quantification of Aβ burden across five brain regions showed no difference between the cognitive groups but regional variability (Figure 3G-H). Next, we sought to investigate glia, integral to normal brain function, in relation to lifetime cognitive performances within the HA cohort. Immunohistochemistry imaging shows CD68 burden is increased in the LCD group across all five brain regions (Figure 3G-I) however quantification only shows an significance increase in the LCD hippocampal region suggesting activated microglia may be a factor in resilience to cognitive ageing. GFAP immunolabelling showed no regional and/or group differences (Figure 3G-J). P-Tau burdens display regional variation and increases in P-Tau burdens were associated with APOE carriers (Figure 3G-K).

RNA sequencing of biochemically isolated synaptoneurosomes reveals 363 synaptic DEG's (< FDR 0.05) between LCR and LCD cohorts in BA20/21 (Figure 4A) and 1116 DEGs in synapses from BA17 (Figure 4C). These changes were not reflected at the protein level, which showed no DEP's < FDR 0.05 were identified (DOI Table S2). In the total brain homogenate fraction, transcriptional changes were more limited suggesting altered transport of RNA to synapses. (Figure 4B, D). Only one DEG from total homogenates of BA20/21 was also significantly changed at the protein level, namely acyl-CoA synthetase family member 2 (ACSF2) (FDR < 0.05, DOI Table S2). In BA17, similarly only a single DEP, serine and arginine rich splicing factor 7 (SRSF7) was identified (FDR < 0.05, DOI Table S2) and expression was increased in the LCR cohort. The top 25 biological pathways identified from transcriptional changes across both brain regions and sample preparations were similar (Figure 4E). Interestingly, canonical pathways associated with neurotransmission and memory were inhibited or decreased in the LCR cohort, irrespective of region. Activated or increased pathways were limited (orange) and were asso-

ciated with stress and immune response. These data compliment gene ontology pathways identified which also showed neurotransmission related pathways such as synaptic vesicle exocytosis, post-synaptic activity, neurotransmitter secretion were all down in the LCR cohort (DOI Folder S3). Pathways activated or increased were associated with ribosomal and transcriptional processes. The synaptogenesis signaling pathway was ranked highest across all sample and regional cohorts (Figure 4E) and was decreased in the LCR group. As shown in Figure S4, this pathway is involved many complex biological interactions at both pre and post-synaptic terminals. CDK5 signaling was ranked 25th on the IPA canonical heatmap (Figure 4E), and as illustrated in Figure S5, this pathway shows Tau is downregulated in the LCR cohort. Regulation of tau through this pathway may be protective here in the LCR cohort. Together these data indicate that despite similar synapse densities and synaptic accumulation of tau and Aβ, levels of transcripts involved in synaptic signaling are decreased in synapses of people who have maintained cognition, indicating that resilience to pathology-induced hyperactivity may be protective against cognitive decline.

iPSC-neuron model from LCR and LCD cognitively resilient individuals reveals dampening of synaptic gene expression in response to challenge with human Aβ in lifetime cognitive resilient neurons compared to neurons from individuals with lifetime cognitive decline.

To explore whether dampening of synaptic gene expression in resilient individuals observed post-mortem could be at least in part due to genetic factors, we used iPSC lines generated from blood cells of LBC1936 participants with known cognitive ageing status[31] (Figure 5A). iPSC-derived cortical neurons were matured for 60 days post-final passage then challenged with human brain homogenate containing soluble Aβ to model exposure of neurons to low levels Aβ during ageing in line with our observations of amyloid deposition in both LCR and LCD brains (Figure 3). To specifically assess the effect of Aβ on the synaptic structure and neuronal protein expression, we also exposed cultures to the same brain homogenate immunodepleted for Aβ (Aβ-) for 48 h (Figure 5B). Quantification of post-synaptic marker homer1 co-localized with dendritic maker MAP2 showed no difference in synaptic density between LCR and LCD lines (LCR Aβ- and Aβ+ four cases; LCD Aβ- and Aβ+ two cases), regardless of treatment condition (Figure 5C), supporting previous AT findings in PM tissue (Figure 3B). On a transcriptional level, some genes identified in PM tissue were also present in the iPSC-neuronal model. Interestingly, in LCR iPSC-neurons *SNAP25* and *SYT1* expression decreases in response to Aβ challenge

ratio = 2.88; *p* = 0.01, d = 63). Presynaptic tau accumulation was significantly increased in AD (G, F[2,32.41] = 25.50, *p* < 0.0001) and significantly higher in BA20/21 than in BA17 (F[1,135.23] = 25.69, *p* < 0.001). There was also a significant interaction between cohort and brain region (F[2,127.08] = 5.75, *p* = 0.004). Pairwise post-hoc comparisons showed a significant increase in presynaptic tau accumulation in AD in comparison to ML and HA cohorts and this was evident in both regions (BA20/21, ML v AD (t ratio = 5.67; *p* < 0.0001, d = 64); HA v AD (t ratio = 6.75; *p* < 0.0001, d = 52); BA17, ML v AD (t ratio = 3.95; *p* = 0.0006, d = 56); HA v AD (t ratio = 3.95; *p* = 0.0007, d = 50). Postsynaptic tau accumulation increases from ML to HA to AD groups (H, F[2,31.81] = 28.65, *p* < 0.0001) and is higher in BA20/21 than BA17 (F[1,135.56] = 31.78, *p* < 0.001). There is also an interaction between brain region and cohort (F[2,126.91] = 7.83, *p* = 0.0006). Pairwise post-hoc comparisons showed a significant increase in postsynaptic tau accumulation in AD in comparison to ML and HA cohorts and this was evident in both regions (BA20/21, ML v AD (t ratio = 5.92; *p* < 0.0001, d = 63); HA v AD (t ratio = 7.40; *p* < 0.0001, d = 52); BA17, ML v AD (t ratio = 4.13; *p* = 0.0004, d = 55); HA v AD (t ratio = 4.15; *p* = 0.0004, d = 50). For box-plots, each point represents case medians. Type III ANOVA with Satterthwaite correction were performed on the linear mixed effects models. Scale bar 1 μm for IMARIS reconstructions. * Represent *p* < 0.05 post-hoc comparisons
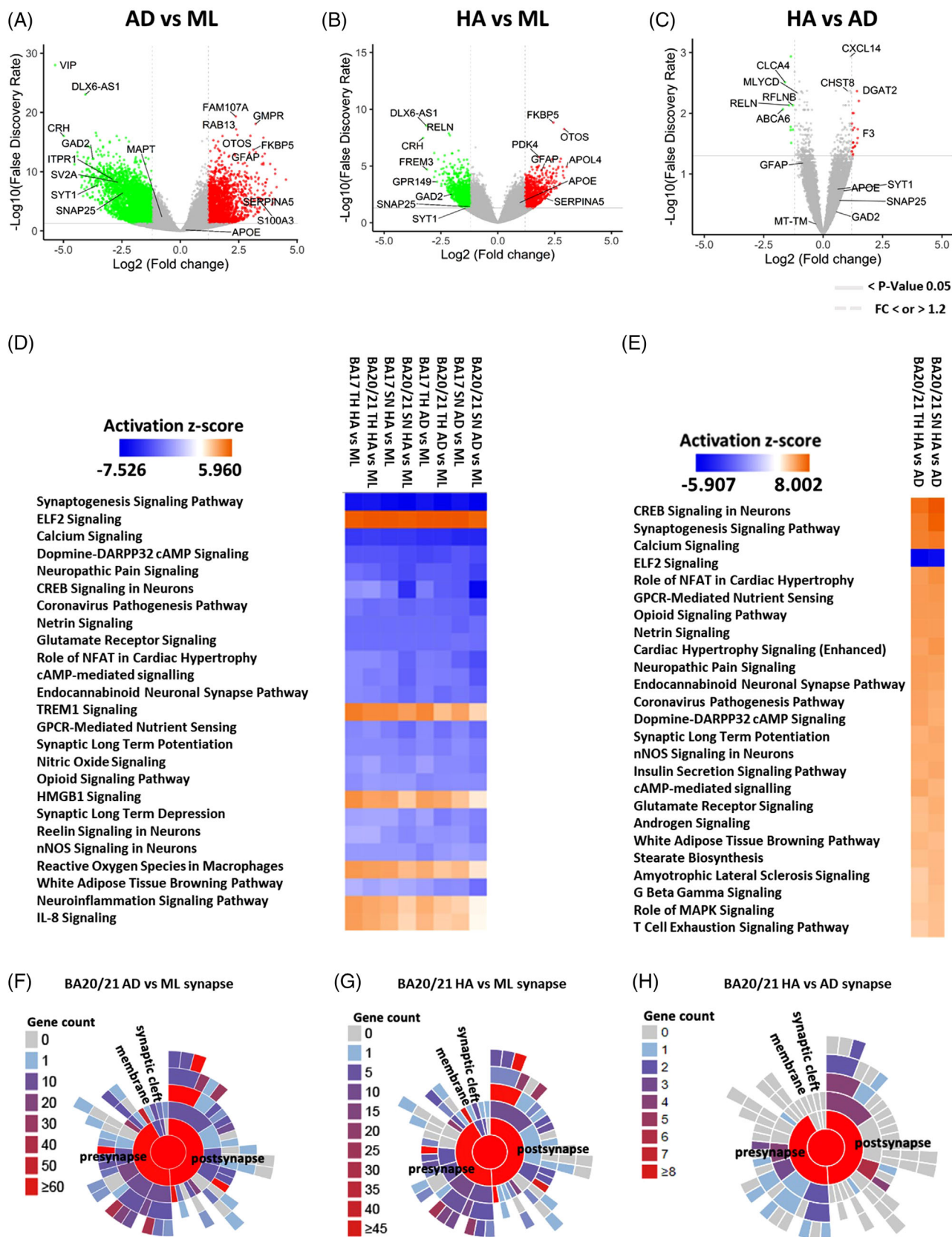
FIGURE 2 Molecular changes in synapses in healthy ageing (HA) and AD indicate decreased synaptic function and increased inflammation compared to mid-life (ML). (A) Comparing BA20/21 synaptic (synaptoneurosome) transcriptional changes between AD versus ML highlights many differentially expressed genes (9671 DEG's < FDR 0.05). (B) 5801 DEGs with FDR < 0.05 between HA and ML. (C) Fewer transcriptional changes are observed between HA and AD (293 DEG's < FDR 0.05). (D) Top 25 canonical pathways associated with total homogenate (TH) and

compared to Aβ- challenge and these synaptic genes are also shown to decrease in PM tissue (Figure 4A-C) in the LCR cohort. The fact that no differences in *TM4SF1* expression were detected (Figure 5F) shows that not all synaptic genes are necessarily affected by these experimental conditions in vitro and therefore that not all of the susceptibility to the response to the ageing brain environment are genetically encoded.

4 | DISCUSSION

In this study, we present detailed characterization of post-mortem brain differences in young people, healthy agers, and people with AD at the structural and molecular level. We observed a decrease in paired synaptic densities between young controls (ML) and people with Alzheimer's disease (AD). There was a reduction of synapses between HA and ML cohorts also in BA17 but not BA20/21. This may be expected as during this normal ageing process only a slight reduction in synaptic numbers of between 10% to 15% is anticipated after 65 years of age.[36] A stepwise increase in the proportion of remaining synapses containing amyloid beta or tau proteins was also evident, which was more pronounced in BA20/21 than BA17 as expected from the known distribution of pathology in AD. A stepwise increase in GFAP burden between ML, HA and AD was expected as GFAP increases progressively with ageing and cognitive decline.[37] This increase could also be in response to Aβ burden although higher levels of GFAP burdens seen in hippocampus regions across all cohorts do not mirror Aβ burdens in the same region comparison suggesting other factors were at play. Previous studies investigating DNA methylation signatures in the LBC1936 cohort have indicated CD68 burdens are highest in the hippocampal brain region.[38] Here we again show evidence of this neuroimmune response; however, changes did not reach significance in this region unlike regions BA20/21 and BA46. A more pronounced increase in P-Tau burden in AD in comparison to ML and HA was anticipated as abnormal tau increases progressively with cognitive decline.[39]

Collectively, these preliminary data highlight the importance of using more than one brain region for investigations as regional differences in burdens can vary, and this may be due to many factors such as cognitive processing demands of that region, pathological load and disease stage.

In addition to pathological studies, we examined RNA and proteins isolated from the same tissue, with the hope of discovering novel biological processes associated with cognitive decline. Our analysis shows limited correlations between both RNA and protein datasets as has been described.[40] One potential explanation for this discrepancy is that large numbers of transcripts are not translated to proteins or are transcribed, but some may be expressed below the detection limit of proteomics. Protein abundance is also controlled by other factors such as post-transcriptional regulation, modifications, and degradation, independent to mRNA abundance. Our transcriptomic data were broadly similar to a study comparing AD to control brain tissue[41] (Figure S6); however here we extend to analysis of synaptic transcripts. Our data indicate that molecular pathways important for synapse function decrease from midlife to ageing to AD and conversely that stress and inflammation pathways increase from midlife to ageing to AD. Several genes of interest were identified including *RRAS*, which is involved in axon guidance, angiogenesis and synaptic function and plasticity.[42] *RRAS* was increased in AD in comparison to ML, possibly to protect neurons from neurodegeneration. In contrast, *ITPR1*, a receptor that mediates calcium release from the endoplasmic reticulum[43] was downregulated in AD in comparison to ML. *GAD2* an enzyme involved in the synthesis of the major inhibitory neurotransmitter, γ-aminobutyric acid (GABA) and therefore present in GABAergic inhibitory neurons and synaptic terminals was also downregulated in AD versus ML. These data support our recent findings showing significant decreases in inhibitory neuron and synapse density in AD.[44] Earlier studies in our lab have shown CLU is increased in AD[10] supporting genome wide association studies that previously identified the protein as an additional risk factor involved in AD.[45] Here, we show CLU is upregulated in AD in comparison to ML controls. Interestingly, direct comparison between HA versus AD show no evidence of transcriptional changes in BA17. This implies the BA17 brain region in AD had a similar transcript profile to a healthy aged brain, regardless of dementia status which, supports previous studies showing the visual cortex is affected relatively late in the disease process.[46] Synaptic densities were also in the same range between HA and AD in the BA17 region, supporting this observation. These data again highlight the importance of using more than one brain region for investigations as regional differences in transcriptional expression can vary. The majority of activated canonical pathways in BA20/21 in HA versus AD were associated with

---

synaptoneurosome (SN) brain preparations across both brain regions (BA17 and BA20/21) display similar profiles between HA or AD to ML cohorts. An inhibition or a decrease of canonical pathways (blue) associated with neurotransmission and memory is evident in both HA and AD in comparison to ML cohorts. Stress and immune response pathways appear to be activated (orange) or increased in both HA and AD in comparison to ML. (E) The top 25 canonical pathways associated with TH and SN brain preparations in BA20/21 between HA versus AD (BA17 showed no differences) show a decrease in only one biological pathway (blue) associated with stress response, whilst remaining canonical pathways associated with neurotransmission and memory were all increased (orange) in HA cohort. (F) 894 of the DEGs between AD and ML cohorts in BA20/21 synapses mapped to known synaptic proteins in the SynGO annotated database. 467 of these DEGs were associated with the post-synapse and 401 with the pre-synapse. (G) In HA versus ML BA20/21 synapses, 615 genes were mapped to SynGO of which 337 were associated with the post-synapse and 285 with the pre-synapse. (H) From the 293 transcripts identified in synapses of BA20/21 (HA vs. AD), an even number of both pre and post-synaptic genes (*n* = 24) were identified using SynGo curated database, highlighting both synapse domains were adapting equaling in the healthy agers and/or not adapting in the AD brains. A-C show Volcano plots of log2 fold change versus -log10 of the false discovery rate. Genes above solid grey line on volcano plots show FDR = 0.05 and dotted lines log2 fold change 1.2 (red) and -1.2 (green) respectively. Transcripts of interest are labelled in black
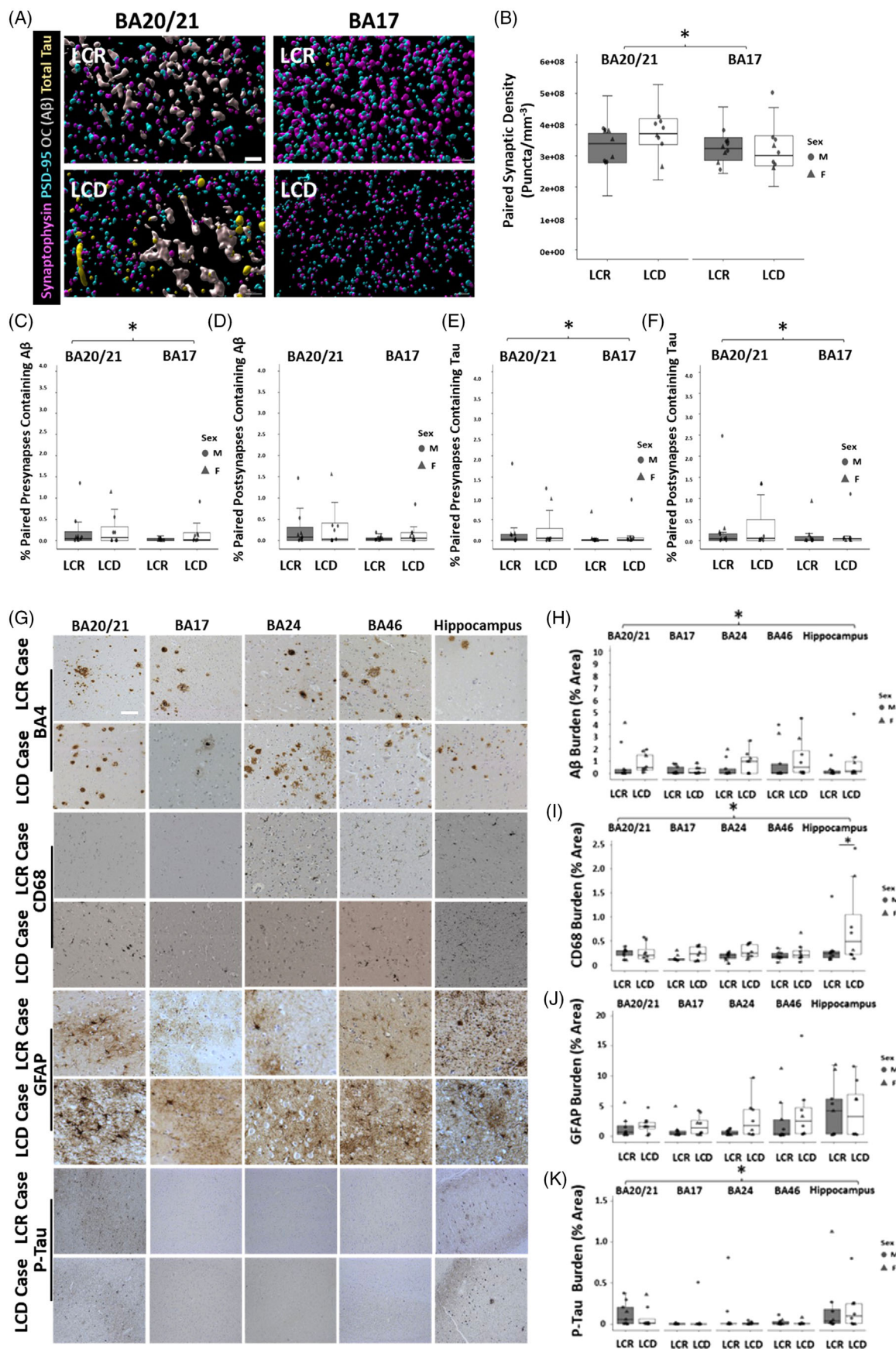
FIGURE 3 Maintained synaptic density and increased gliosis in people with lifetime cognitive decline. (A) Representative 3D reconstructions of AT stacks from Lifetime cognitive resilient (LCR) and Lifetime cognitive decline (LCD) cohorts. Serial sections of 70 nm sections from BA20/21

neurotransmission and memory, and included biological pathways such as CREB, synaptogenesis, calcium, LTP, and glutamate receptor signaling.

Within our HA cohort, age-adjusted longitudinal MHT scores were used to sub-categorize samples into a Lifetime cognitive resilient (LCR) group and a Lifetime cognitive decline (LCD) group. We acknowledge here the further subsetting of these samples into smaller sizes confers risks for unreliable detection of effects due to low statistical power. Nevertheless, life course cognitive data plus post-mortem brain is rare, and characterizing changes in brain structure in both groups will further our understanding of healthy brain ageing and cognitive decline. There was no change in synapse density between people with age-related cognitive decline in the absence of dementia in either BA20/21 or BA17. It is possible more subtle differences are occurring that are not detectable by AT. Stereological assessment of CD68 burdens between LCR and LCD groups highlight activated microglia increase with poorer cognitive status in the hippocampus region. In addition to gliosis, we observed molecular changes in synapses between LCR and LCD tissue. Interestingly, in BA17 one of the major biological themes identified from our transcriptomic analysis in IPA was Bruton's tyrosine kinase (BTK). BTK elevation is found in AD mouse models and human AD brains and is associated with a neuroinflammatory response to extracellular Aβ accumulation and or synaptic loss [98]. BTK is also a known regulator of microglial phagocytosis, and inhibition of BTK signaling is known to decrease microglial uptake of synaptosomes and thus may play a role in maintaining and/or improving cognition [98]. Here, BTK was decreased in the LCR cohort. Therefore, manipulating BTK by using BTK inhibitors may provide a promising strategy moving forward to encourage healthy ageing. Collectively, these data suggest activated phagocytic microglial activity is detrimental to healthy ageing. Biological pathways associated with both regions in LCR and LCD groups indicate damping synapse activity in the more cognitively resilient cohort. We know hyperexcitability is an early signature of neuronal and cognitive dysfunction and studies in animal models have indicated hyperactivity in selective circuits driven by pathologies such as oligomeric Aβ can contribute to cognitive impairment.[47] Both Aβ and tau secretion are also increased with neuronal activity thus dampening activity may essentially slow the accumulation or spread of pathological proteins like soluble oligomers that could drive the gliosis we observe in the LCD group. Modulating this brain hyperexcitabil-

ity, known to be elevated in people with AD, therefore may provide a novel therapeutic approach to improve cognition and/or long-term cognitive resilience. The current investigation of anti-seizure drugs as treatments for AD[48] may thus also be beneficial in preventing cognitive decline during healthy ageing. These findings could be interpreted to contrast with the idea of cognitive reserve and the protective effect of education against developing dementia. However, it could be the case that enriching activities like education make neural circuits more efficient. An example of this comes from a functional magnetic resonance imaging (fMRI) study measuring the brain activity of professional versus naïve piano players.[49] Here brain activation was found to be lower in the professional pianists suggesting this dampening effect may be beneficial to the brain as energy requirements would be less whilst performing these most complex activities. Our transcriptional data provide a valuable resource of genes to target to support cognitive resilience by lowering synaptic activity. However, one would have to be cautious whilst using drugs to instate these neuronal damping changes and future trials will establish if specific drug treatments are safe, tolerable and effective for memory function stabilization. Neuromodulation technologies to enhance or suppress activity of the neurons is another promising approach in its infancy with hopes of providing superior therapeutics for many cognitive disorders.[50]

5 | LIMITATIONS

This study has several limitations. Firstly, synaptoneurosomes (SN) may contain small amounts of non-synaptic material such as neuronal, glial and myelin contaminants; however they have the advantage of containing both the presynaptic terminal and postsynaptic spine head, which is often excluded in more "pure" synaptic preparations. Secondly, cognitive data was only available for the healthy aging group and there was variability between the last cognitive test and death, which was several years in some cases. Thirdly, iPSC-derived neurons represent a developmentally young and reductionist model of tissue complexity, making direct comparison of results with post-mortem tissue difficult. Despite this, synaptic genes relevant to post-mortem data were expressed in iPSC-neurons and form a basis for further exploitation in future experiments. Lastly, we acknowledge the sample sizes, particularly of the healthy agers split by cognition, are low and may be prone to both

and BA17 were stained for synaptophysin (magenta), PSD95 (cyan), OC (grey) and Total tau (yellow). (B) Synapse density was lower in BA17 than BA2021 (F[1,133.40] = 4.05, p = 0.04); however there was no difference in excitatory synapse density between cognitive cohorts (F[1, 12.50] = 0.51, p = 0.48). There was similarly no difference between LCR and LCD in the percent pre or post synapses containing Aβ or tau, but co-localization Aβ or tau with synapses showed regional increases in BA20/21 in comparison to BA17 (C F[1,110.53] = 4.84, p = 0.02; E F[1,89.94] = 6.38, p = 0.01; F F[1,88.17] = 4.67, p = 0.03). G Representative images of Aβ (BA4), microglia (CD68), astrocytes (GFAP), and P-Tau (AT8) are shown from all five brain regions, BA20/21, BA17, BA24, BA46, and hippocampus across LCR and LCD groups. (H) Aβ burden measurements plotted across five brain regions show regional variation in Aβ burdens between both groups (F[4,60.00] = 3.80, p = 0.007) and an increase in APOE4 carriers (F[1,11.50] = 15.55, p = 0.002). (I) CD68 burden measurements show a significant increase in microglial burden in the LCD group (F[4,60.00] = 4.04, p = 0.005) which reaches post-hoc pairwise significance in hippocampus (t ratio = 2.25; p = 0.02, d = 54). (J) GFAP burdens show no significant changes between groups or regions. (K) P-Tau burdens plotted across five brain regions show regional variation in P-Tau burdens between both groups (F[4,59.31] = 6.77, p = 0.0001) and an increase in APOE4 carriers (F[1,12.04] = 8.64, p = 0.01). For box-plots, each point represents case medians. Type III ANOVA with Satterthwaite correction were performed on the linear mixed effects models. Scale bar 5 μm for IMARIS reconstructions, 150 μm for IHC images. * Represent p < 0.05 post-hoc comparisons
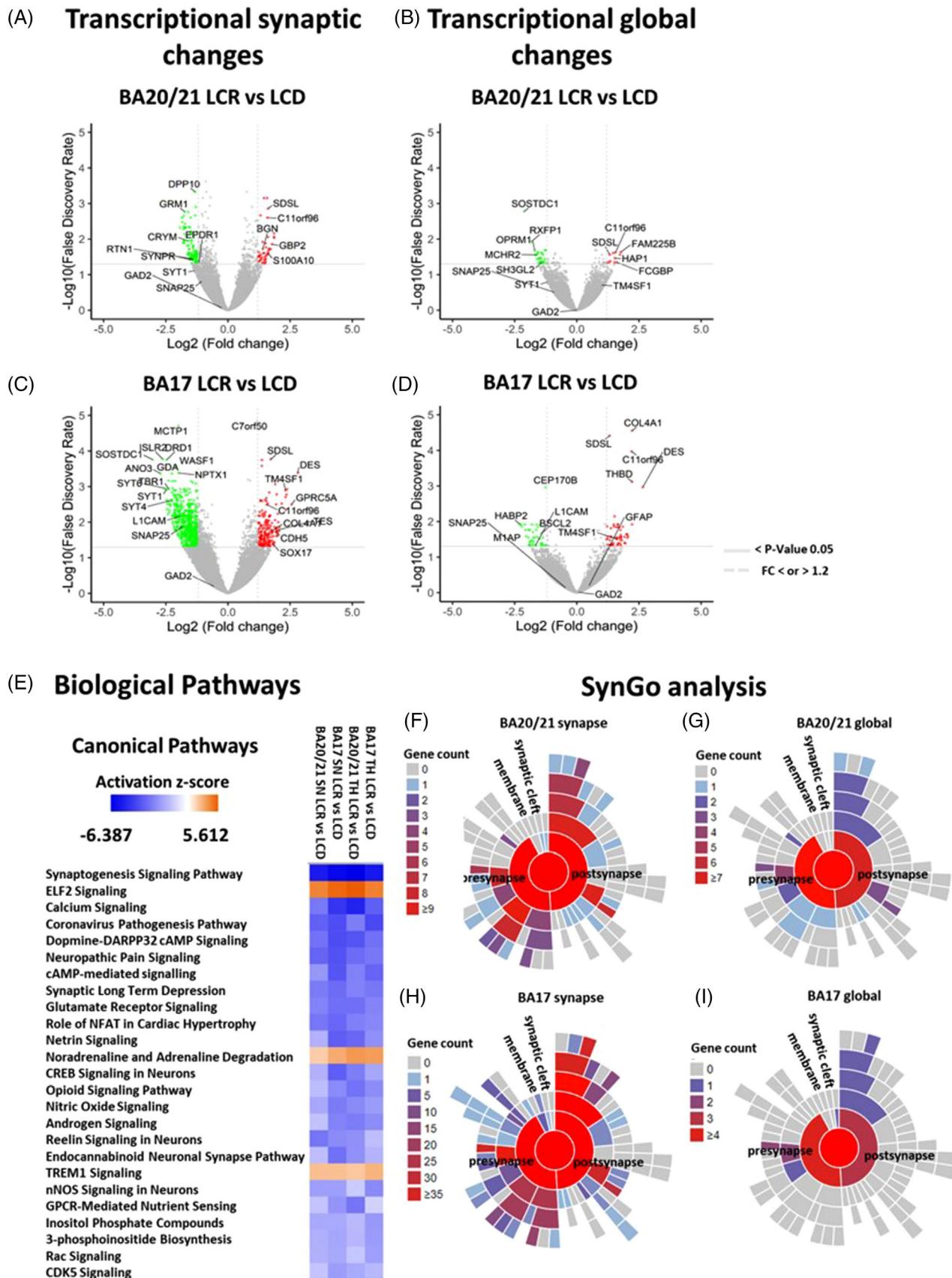
FIGURE 4 People with lifetime cognitive resilience have dampened synaptic signaling pathways. (A) 363 DEG's (< FDR 0.05) were found when comparing transcription at the synapse in brain region BA20/21 between LCR and LCD cohorts. (B) Fewer DEG's (75, < FDR 0.05) were observed in the total homogenate fraction. (C) In BA17, 1116 DEG's < FDR 0.05 were identified between cognitive groups. (D) This was not reflected at a

type 1 and 2 statistical errors; however, the study is a valuable addition to the field using a well-characterized set of subjects with cognitive data from childhood, brain tissue, and iPSC availability. Despite these limitations, the data albeit preliminary presented here are a comprehensive examination of synaptic changes in a unique cohort of ageing participants. In summary, we observe that between midlife, healthy ageing, and Alzheimer's disease, there is substantial gliosis, synapse loss, synaptic accumulation of pathology, and lower levels of transcripts

global level where only 112 DEG's were identified. (E) The top 25 canonical pathways changes indicate decreases in abundance (blue) of many pathways involved in synaptic function including neurotransmission and memory in people with lifetime cognitive resilience. Increased pathways (orange) were associated with stress and immune responses. (F) When looking at transcripts in the synapses of BA20/21, there are 363 DEGs of which 27 are known pre-synaptic genes and 27 are known post-synaptic genes in the SynGo curated database. The majority of these (23 of each) are downregulated. (G) SynGo analysis of the 75 DEGs in total homogenate of BA20/21 shows that people with better cognition had alterations in 10 synaptic genes, of which nine are pre-synaptic and seven were post-synaptic highlighting overlap between synaptic genes identified. (H) In BA17 synaptic fractions, there are 107 pre-synaptic and 106 post-synaptic genes changed. Of these, the vast majority (103 pre, 102 post) are downregulated. (I) In total four pre-synaptic and three post-synaptic specific genes were altered in total homogenate of BA17 between the cognitive groups. Volcano plot of log2 fold change versus -log10 of the false discovery rate. Genes above solid grey line on volcano plots show FDR = 0.05 and dotted lines log2 fold change 1.2 (red) and -1.2 (green) respectively. Transcripts of interest are labelled in black
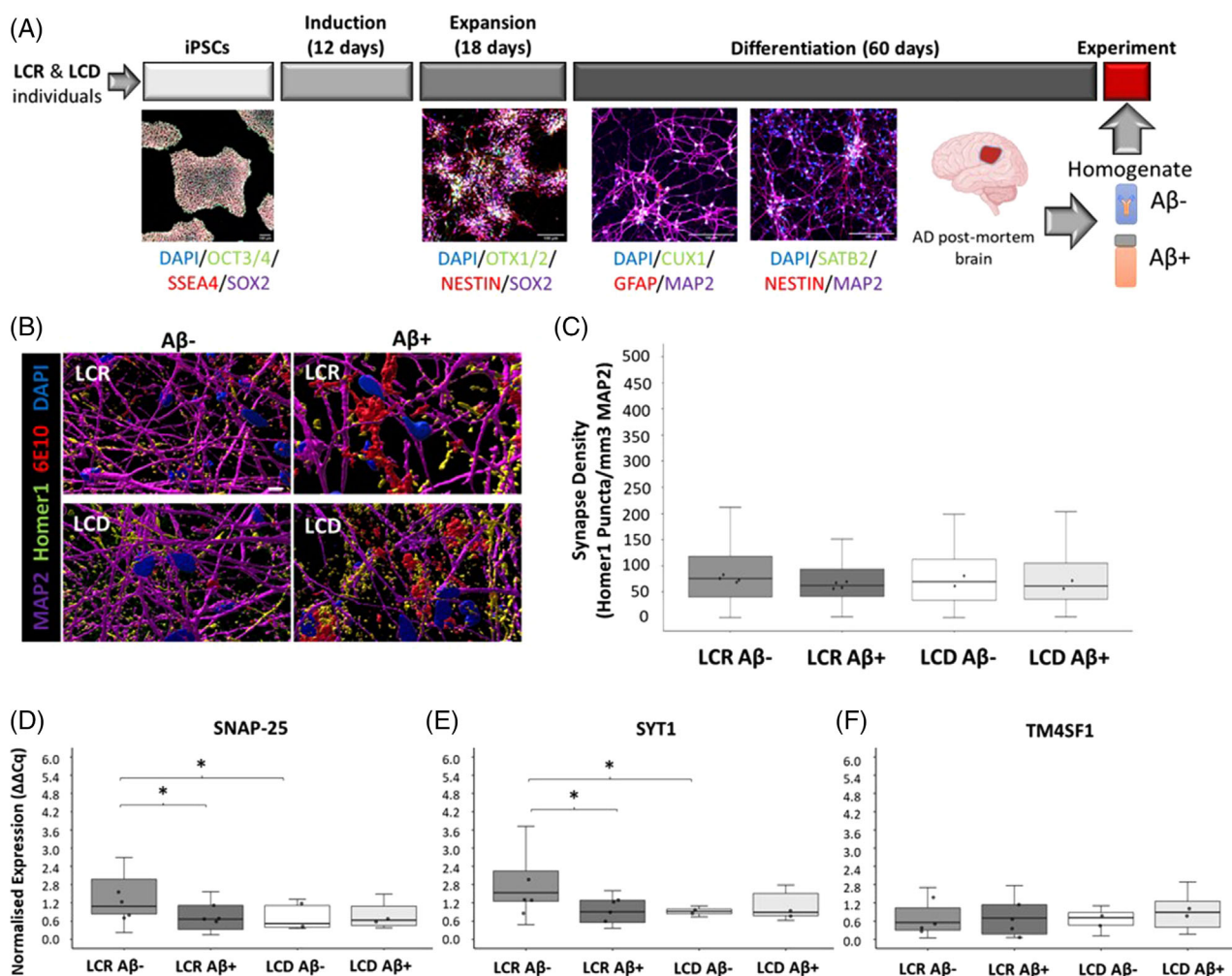

FIGURE 5 iPSC-derived neurons from LCR individuals have decreased expression of synaptic genes in response to Aβ challenge. (A) Overview of the process by which iPSCs from LCR and LCD individuals were differentiated to cortical neurons. Human AD brain homogenate enriched (Aβ+) or immunodepleted (Aβ-) for soluble Aβ42 was added to cells at experiment time point. (B) Representative 3D reconstructions showing the effect of homogenate treatment on LCD and LCR neurons. (C) Automated quantification of homer1 puncta (post-synaptic density) colocalized with MAP2 (dendrites) showed no significant difference between Aβ treatment or cell line group. (D-E) RT-qPCR revealed that *SNAP-25* and *SYT1* expression significantly differed between Aβ treatments in the Lifetime Cognitive Resilient (LCR) group, but not in the Lifetime Cognitive Decline (LCD) group. (F) No difference between treatment or lifetime cognitive ageing groups was observed in *TM4SF1* expression. For box-plots, each point represents case medians. Type III ANOVA with Satterthwaite correction were performed on the linear mixed effects models. Scale bar 100 μm (A), 5 μm for IMARIS reconstructions (B). * Represent $p < 0.05$ post-hoc comparisons

involved in synaptic function. In healthy aged participants without dementia, gliosis was associated with cognitive decline, but in contrast to the AD data, lower levels of gene expression associated with synaptic signaling were paradoxically associated with resilience to cognitive decline. This surprising result has implications for preventing cognitive decline in ageing that will be different from treating people with AD. Together our data indicate that synaptic resilience plays an important role in maintaining cognition during ageing. Future directions will include using the iPSC neuronal model presented in this paper and other model systems to search for interventions to reverse molecular changes described in this study that are assicated with cognitive decline in ageing and Alzheimer's disease.

CONFLICT OF INTEREST

TSJ received collaborative grant funding from an anonymous industry partner for this work. TSJ is on the scientific advisory board of Cognition Therapeutics, receives honoraria for talks from academic and industry, and is a trustee of two charities: the Guarantors of Brain and the British Neuroscience Association.

REFERENCES

1. Liu X, Abudukeremu A, Jiang Y, et al. Fine or gross motor index as a simple tool for predicting cognitive impairment in elderly people: findings from The Irish Longitudinal Study on Ageing (TILDA). *J Alzheimers Dis.* 2021;83:889-896.
2. Pedersen R, Geerligs L, Andersson M, et al. When functional blurring becomes deleterious: reduced system segregation is associated with less white matter integrity and cognitive decline in aging. *Neuroimage.* 2021;242:118449.
3. Tucker-Drob EM, Brandmaier AM, Lindenberger U. Coupled cognitive changes in adulthood: a meta-analysis. *Psychol Bull.* 2019;145(3):273-301.
4. Nilsson L-GR, Adolfsson R, BÃ¤ckman L, De Frias CM, Molander Bo, Nyberg L. Betula: a prospective cohort study on memory, health and aging. *Aging, Neuropsychology, and Cognition.* 2004;11(2-3):134-148.

5. Morrison JH, Baxter MG. The ageing cortical synapse: hallmarks and implications for cognitive decline. *Nat Rev Neurosci.* 2012;13(4):240-250.
6. Scheff SW, Price DA, Schmitt FA, Mufson EJ. Hippocampal synaptic loss in early Alzheimer's disease and mild cognitive impairment. *Neurobiol Aging.* 2006;27(10):1372-1384.
7. Terry RD, Masliah E, Salmon DP. Physical basis of cognitive alterations in Alzheimer's disease: synapse loss is the major correlate of cognitive impairment. *Ann Neurol.* 1991;30.
8. Dekosky ST, Scheff SW. Synapse loss in frontal cortex biopsies in Alzheimer's disease: correlation with cognitive severity. *Ann Neurol.* 1990;27(5):457-464.
9. Koffie RM, Hashimoto T, Tai H-C, et al. Apolipoprotein E4 effects in Alzheimer's disease are mediated by synaptotoxic oligomeric amyloid-β. *Brain.* 2012;135(7):2155-2168.
10. Jackson RJ, Rose J, Tulloch J, Henstridge C, Smith C, Spires-Jones TL. Clusterin accumulates in synapses in Alzheimer's disease and is increased in apolipoprotein E4 carriers. *Brain Commun.* 2019;1(1).
11. Pickett EK, Herrmann AG, Mcqueen J, et al. Amyloid beta and tau cooperate to cause reversible behavioral and transcriptional deficits in a model of Alzheimer's disease. *Cell Rep.* 2019;29(11):3592-3604.e5. e5.
12. Spires-Jones TL, Hyman BT. The intersection of amyloid beta and tau at synapses in Alzheimer's disease. *Neuron.* 2014;82(4):756-771.
13. Bennett DA, Buchman AS, Boyle PA, Barnes LL, Wilson RS, Schneider JA. Religious orders study and rush memory and aging project. *J Alzheimers Dis.* 2018;64(s1):S161-S189.
14. A Bennett D, A Schneider J, Arvanitakis Z, S Wilson R. Overview and findings from the religious orders study. *Curr Alzheimer Res.* 2012;9(6):628-645.
15. Lv Y, Mao C, Yin Z, Li F, Wu X, Shi X. Healthy ageing and biomarkers cohort study (HABCS): a cohort profile. *BMJ Open.* 2019;9(10):e026513.
16. Bennett HQ, Kingston A, Spiers G, et al. Healthy ageing for all? Comparisons of socioeconomic inequalities in health expectancies over two decades in the Cognitive Function and Ageing Studies I and II. *Int J Epidemiol.* 2021;50(3):841-851.
17. Corley J, Cox SR, Deary IJ. Healthy cognitive ageing in the Lothian Birth Cohort studies: marginal gains not magic bullet. *Psychol Med.* 2018;48(2):187-207.
18. Welstead M, Luciano M, Muniz-Terrera G, Taylor AM, Russ TC. Prevalence of mild cognitive impairment in the Lothian Birth Cohort 1936. *Alzheimer Dis Assoc Disord.* 2021.
19. Racine Maurice SP, HÃ©Bert A, Turcotte V©R, Potvin O, Hudon C, Duchesne S. Childhood socioeconomic status does not predict late-life cognitive decline in the 1936 Lothian Birth Cohort. *Front Psychol.* 2021;12:679044.
20. Harris SE, Cox SR, Bell S, et al. Neurology-related protein biomarkers are associated with cognitive ability and brain volume in older age. *Nat Commun.* 2020;11(1):800.
21. Stevenson AJ, Mccartney DL, Harris SE, et al. Trajectories of inflammatory biomarkers over the eighth decade and their associations with immune cell profiles and epigenetic ageing. *Clin Epigenetics.* 2018;10(1):159.
22. Kay KR, Smith C, Wright AK, et al. Studying synapses in human brain with array tomography and electron microscopy. *Nat Protoc.* 2013;8(7):1366-1380.
23. Henstridge CM, Jackson RJ, Kim JM, et al. Post-mortem brain analyses of the Lothian Birth Cohort 1936: extending lifetime cognitive and brain phenotyping to the level of the synapse. *Acta Neuropathol Commun.* 2015;3(1):53.
24. Tai H-C, Serrano-Pozo A, Hashimoto T, Frosch MP, Spires-Jones TL, Hyman BT. The synaptic accumulation of hyperphosphorylated tau oligomers in Alzheimer disease is associated with dysfunction of the ubiquitin-proteasome system. *Am J Pathol.* 2012;181(4):1426-1435.

25. Sticker A, Goeminne L, Martens L, Clement L. Robust summarization and inference in proteome-wide label-free quantification. *Mol Cell Proteomics*. 2020;19(7):1209-1219.

26. Tebbe A, Klammer M, Sighart S, Schaab C, Daub H. Systematic evaluation of label-free and super-SILAC quantification for proteome expression analysis. *Rapid Commun Mass Spectrom*. 2015;29(9):795-801.

27. Love MI, Huber W, Anders S. Moderated estimation of fold change and dispersion for RNA-seq data with DESeq2. *Genome Biol*. 2014;15(12):550.

28. Wu Di, Smyth GK. Camera: a competitive gene set test accounting for inter-gene correlation. *Nucleic Acids Res*. 2012;40(17):e133-e133.

29. Ritchie ME, Phipson B, Wu Di, et al. limma powers differential expression analyses for RNA-sequencing and microarray studies. *Nucleic Acids Res*. 2015;43(7):e47.

30. Alexa A, Rahnenfuhrer J, Lengauer T. Improved scoring of functional groups from gene expression data by decorrelating GO graph structure. *Bioinformatics*. 2006;22(13):1600-1607.

31. Toombs J, Panther L, Ornelas L, et al. Generation of twenty four induced pluripotent stem cell lines from twenty four members of the Lothian Birth Cohort 1936. *Stem Cell Res*. 2020;46:101851-101851.

32. Shi Y, Kirwan P, Livesey FJ. Directed differentiation of human pluripotent stem cells to cerebral cortex neurons and neural networks. *Nat Protoc*. 2012;7(10):1836-1846.

33. Hong W, Wang Z, Liu W. Diffusible, highly bioactive oligomers represent a critical minority of soluble Aβ in Alzheimer's disease brain. *Acta Neuropathol*. 2018;136(1):19-40.

34. R Core Team, *R: a language and environment for statistical computing*. 2017.

35. Koopmans F, Van Nierop P, Andres-Alonso M, et al. SynGO: an evidence-based, expert-curated knowledge base for the synapse. *Neuron*. 2019;103(2):217-234.e4. e4.

36. Masliah E, Crews L, Hansen L. Synaptic remodeling during aging and in Alzheimer's disease. *J Alzheimers Dis*. 2006;9(3 Suppl):91-99.

37. Sheng JG, Mrak RE, Rovnaghi CR, et al. Human brain S100 beta and S100 beta mRNA expression increases with age: pathogenic implications for Alzheimer's disease. *Neurobiol Aging*. 1996;17(3):359-363.

38. Stevenson AJ, McCartney DL, Gadd DA, et al. A comparison of blood and brain-derived ageing and inflammation-related DNA methylation signatures and their association with microglial burdens. *bioRxiv*. 2020:404228. 2020.11.30..

39. Kent SA, Spires-Jones TL, Durrant CS. The physiological roles of tau and Aβ: implications for Alzheimer's disease pathology and therapeutics. *Acta Neuropathol*. 2020;140(4):417-447.

40. Wang X, Liu Qi, Zhang B. Leveraging the complementary nature of RNA-Seq and shotgun proteomics data. *Proteomics*. 2014;14(23-24):2676-2687.

41. Feng X, Bai Z, Wang J, et al. Robust gene dysregulation in Alzheimer's disease brains. *J Alzheimers Dis*. 2014;41(2):587-597.

42. Qu L, Pan C, He S-M, et al. The Ras superfamily of small GTPases in non-neoplastic cerebral diseases. *Front. Mol. Neurosci*. 2019;12:121-121.

43. Bertini E, Zanni G, Boltshauser E. Chapter 6 - Nonprogressive congenital ataxias. In: Manto M and Huisman TAGM, eds. *Handbook of Clinical Neurology*. Elsevier; 2018:91-103.

44. Kurucu H, Colom-Cadena M, Davies C, et al. Inhibitory synapse loss and accumulation of amyloid beta in inhibitory presynaptic terminals in Alzheimer's disease. *Eur J Neurol*. 2021.

45. Harold D, Abraham R, Hollingworth P, et al. Genome-wide association study identifies variants at CLU and PICALM associated with Alzheimer's disease. *Nat Genet*. 2009;41(10):1088-1093.

46. Cui J-G, Hill JM, Zhao Y, Lukiw WJ. Expression of inflammatory genes in the primary visual cortex of late-stage Alzheimer's disease. *Neuroreport*. 2007;18(2):115-119.

47. Toniolo S, Sen A, Husain M. Modulation of brain hyperexcitability: potential new therapeutic approaches in Alzheimer's disease. *Int J Mol Sci*. 2020;21(23):9318.

48. Cumbo E, Ligori LD. Levetiracetam, lamotrigine, and phenobarbital in patients with epileptic seizures and Alzheimer's disease. *Epilepsy Behav*. 2010;17(4):461-466.

49. Haslinger B, Erhard P, Altenmäler E. Reduced recruitment of motor association areas during bimanual coordination in concert pianists. *Hum Brain Mapp*. 2004;22(3):206-215.

50. Cools R, Arnsten AFT. Neuromodulation of prefrontal cortex cognitive function in primates: the powerful roles of monoamines and acetylcholine. *Neuropsychopharmacology*. 2021.

SUPPORTING INFORMATION

Additional supporting information can be found online in the Supporting Information section at the end of this article.